Transport properties of $Bi_{1-x}Sb_x$ alloy thin films grown on CdTe(111)B

Sunglae Cho, Antonio DiVenere, George K. Wong,* and John B. Ketterson†
Department of Physics and Astronomy and Materials Research Center, Northwestern University, Evanston, Illinois 60208

Jerry R. Meyer
Naval Research Laboratory, Code 5613, Washington, D.C. 20375-5338
(Received 12 October 1998)

We have grown $Bi_{1-x}Sb_x$ alloy thin films on CdTe(111)B over a wide range of Sb concentrations ($0 \leqslant x \leqslant 0.183$) using molecular-beam epitaxy. Temperature-dependent electrical resistivity (ρ) and thermoelectric power (S) were studied. We have observed several differences over the bulk system. The 3.5 and 5.1% Sb alloys show semiconducting behavior, and the Sb concentration with maximum band gap shifted to a lower Sb concentration from 15% in bulk to 9%. Based on a simple interpretation of the temperature-dependent resistivity the maximum gap would be 40 meV, which is larger than that observed in bulk alloys. In addition, we have observed that the power factor S^2/ρ peaks at a significantly higher temperature (250 K) than previously reported for the bulk alloy (80 K). Differences between thin film grown on CdTe(111) and bulk alloy may arise from the effects of strain, which is supported by theoretical electronic band calculations. These results show that BiSb films may be useful as band-engineered materials in thermoelectric devices.
[S0163-1829(99)15315-3]

I. INTRODUCTION

Bi and Sb are semimetals with a rhombohedral structure. They have a small energy overlap between the conduction and valence bands, high carrier mobilities, and small effective masses. Because of these properties, Bi and Sb have frequently been used for quantum-size effect studies. The $Bi_{1-x}Sb_x$ alloy system can be either a semiconductor or semimetal depending on the Sb concentration,[1–17] as may be seen from the band structure in Fig. 1. The addition of Sb to Bi causes the L_s and T bands to move down with respect to the L_a band. At $x=0.04$ the L bands invert[2,3] and at $x=0.07$ the overlap between the hole T and L_a bands disappears,[4] resulting in an indirect band-gap semiconductor for $x<0.09$. For $0.09<x<0.15$, $Bi_{1-x}Sb_x$ is a direct gap semiconductor with a maximum band gap in the range 18–20 meV for 12–15% Sb concentration.[1,6,7] For $x>0.15$, the hole H band lies above L_s and we again have an indirect semiconductor. Finally at $x=0.22$, H crosses L_a, and the alloys are again semimetallic up to $x=1$ (pure Sb). In addition, the BiSb band structure depends on temperature, external pressure,[11–15] and magnetic field.[10] With properties such as a small band gap, high mobility, and a reduced lattice thermal conductivity, semiconducting Bi-rich $Bi_{1-x}Sb_x$ alloys may potentially be used as an n-type thermoelement operating around 80 K. The thermoelectric figure of merit, defined by $ZT=(S^2/\rho\kappa)T$, is 0.88 at 80 K in a magnetic field of 0.13 T,[6] where S is the thermoelectric power (TEP) or Seebeck coefficient, ρ is the electrical resistivity, and κ is the thermal conductivity.

There have been several earlier efforts to grow Bi thin films and superlattices. High-vacuum thermal evaporation on mica substrates was originally used to grow epitaxial Bi films,[18] Bi/CdTe superlattices,[19] and Bi/PbTe superlattices.[20] Molecular-beam epitaxy (MBE) was more recently used to grow Bi and BiSb thin films on BaF_2[21–23] and CdTe substrates,[24–28] and superlattices on CdTe substrates.[24,27] Morelli, Partin, and Heremans[16] reported, based on electrical transport measurements, a slight enhancement of the band gap of BiSb alloy thin films for various Sb concentrations grown by MBE on BaF_2(111) substrates. They attributed this to a compressive strain caused by the smaller lattice constant of the substrate. In the present paper, we report a detailed experimental study of the electrical resistivity and thermoelectric properties of $Bi_{1-x}Sb_x$ alloy films grown on CdTe(111)B substrates over a wide range of Sb concentrations ($0 \leqslant x \leqslant 0.183$). X-ray measurements of the thin-film lattice constants allow the effect of strain on the electrical and thermal transport to be assessed.

II. EXPERIMENT

$Bi_{1-x}Sb_x$ alloy thin films with $x=0$, 0.019, 0.035, 0.051, 0.072, 0.088, 0.112, 0.143, 0.164, and 0.183 were grown by

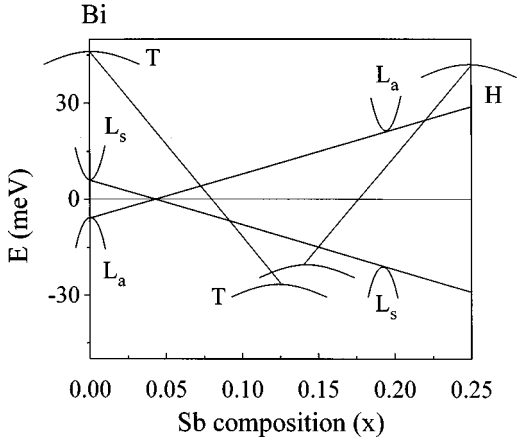

FIG. 1. Variation of energy bands near Fermi level of bulk $Bi_{1-x}Sb_x$ alloys as a function of Sb composition x in the interval $0 \leqslant x < 0.25$.

MBE onto semi-insulating CdTe(111)B substrates. The base pressure of the growth chamber was in the 10^{-10} Torr range. The growth direction of $Bi_{1-x}Sb_x$ on CdTe(111)B is parallel to the trigonal axis. We first deposited a 3000-Å CdTe buffer layer at 250 °C, followed by the $Bi_{1-x}Sb_x$ layer at a rate of 0.4 Å/s and at a growth temperature of 100 °C. $Bi_{1-x}Sb_x$ films were prepared using two effusion cells containing Bi and Sb. To vary the Sb concentration in the alloys, we maintained the Bi cell at 720 °C and changed the Sb cell temperature between 480 and 550 °C. The compositions of alloys were monitored by a quartz crystal microbalence. The accuracy has been confirmed by inductively coupled plasma (ICP) spectroscopy analysis. For the ICP measurements the films were dissolved in 8% dilute nitric acid. Using two known standard concentrations we could determine the sample compositions by interpolation. The error in determining the relative stoichiometry of the material is the instrumental error, $\pm 3\%$ per element (e.g., $x=0.088\pm 0.0026$ for the 8.8% Sb concentration). We used these ICP calibrated values for the Sb concentration in our samples. Reflection high-energy electron diffraction (RHEED) was used to examine the specific surface reconstruction of the deposited layers. The $Bi_{1-x}Sb_x$ epilayers had nominal thicknesses of 1 μm. Since the hexagonal lattice constants of Bi and Sb are 4.546 and 4.308 Å, respectively, the lattice mismatch with CdTe(111)B (4.58 Å) increases from 0.7 to 1.8% between these limits. The structural properties were reported elsewhere.[29]

Films were processed into bar-shape patterns using photolithography and lift-off techniques for electrical measurements. To measure the TEP we used the differential method, in which a small temperature difference is maintained across the sample to produce the thermoelectric voltage: $\Delta V = S\nabla T + b(\nabla T)^2 + \ldots$, where b is a constant. The thermoelectric voltage $(\Delta V)_i$ versus temperature difference $(\nabla T)_i$ were plotted and from the slope of the linear region we could determine the TEP. To measure the temperature difference across the sample, we used a differential Cu-constantan thermocouple. The thermoelectric voltage was measured by using thin copper leads and was later corrected for the TEP of the leads to obtain the final results.[27]

III. RESULTS AND DISCUSSION

The temperature-dependent electrical resistivities of the $Bi_{1-x}Sb_x$ alloy thin films with various Sb compositions are shown in Figs. 2(a) and 2(b). At room temperature, the resistivity differences between the various compositions is small. However, as the temperature decreases the behavior changes significantly. The 1.9% Sb concentration sample shows a slightly increased resistivity at low temperature. As the Sb concentration increases, the resistivity increases rapidly up to 8.8% Sb concentration as shown in Fig. 2(a). It should be noted that the 8.8% Sb alloy has the highest resistivity at low temperature. With the further addition of Sb, the resistivity decreases as shown in Fig. 2(b). The 18.3% Sb alloy shows a slightly increased resistivity at low temperature. Note that at low temperatures the resistivity saturates.

The saturation of the resistivity at low temperature may indicate the existence of an impurity band.[7] In n-type semiconductors, Wannier[31] treated an impurity as a quasihydrogenic atom in a continuous dielectric material with the extra electron bound to a spherically symmetric positive charge embedded in a solid dielectric material. The binding energy of the electron to the impurity atom is then

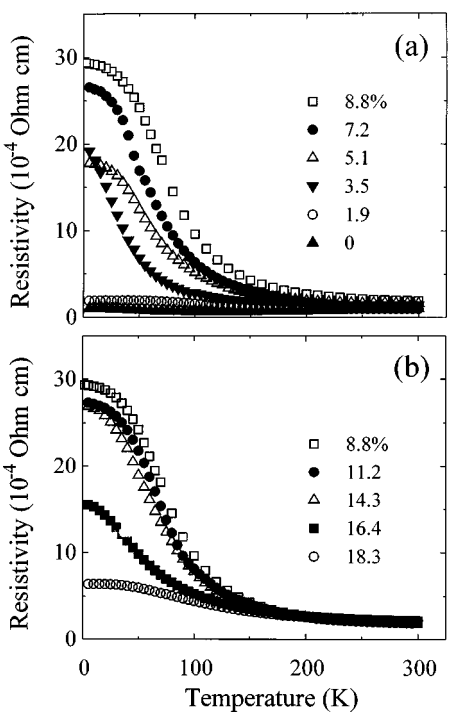

FIG. 2. The temperature dependence of the electrical resistivities of $Bi_{1-x}Sb_x$ alloy thin films grown on CdTe(111)B with various Sb concentrations. The 8.8% Sb alloy was graphed twice for comparison.

$$E_n = -\frac{e^4 m^*}{2n^2\hbar^2\varepsilon^2} \approx -\frac{13.6}{n^2\varepsilon^2}\left(\frac{m^*}{m_0}\right) \text{ eV} \tag{1}$$

and the orbital radius of the electron is

$$r_n = \frac{n^2\hbar^2\varepsilon}{e^2 m}\left(\frac{m_0}{m^*}\right) \approx 0.53\frac{m_0}{m^*}n^2\varepsilon \text{ Å}, \tag{2}$$

where m_0 is the electron rest mass, m^* is the effective mass, and ε is the dielectric constant. The work necessary to separate the electron from the atom is given by

$$\Delta E = E_\infty - E_1 \approx \frac{13.6}{\varepsilon^2}\left(\frac{m^*}{m_0}\right) \text{ eV}. \tag{3}$$

BiSb alloys have a high dielectric constant[32] ($\sim$100) and low effective masses ($\sim 0.01 m_0$). Using Eqs. (2) and (3) yields $\Delta E \sim 1.4\times 10^{-5}$ eV and $r_l \sim 5.3\times 10^3$ Å. In comparison, Si has a $\Delta E \sim (1.0-4.9)\times 10^{-2}$ eV and $r_1 \sim (1.9-3.7)\times 10^1$ Å for $\varepsilon = 11.8$ and $m^*/m = 0.33$. Furthermore, free carriers are expected to screen out the bound state of high doping levels since the screening length is much less than the orbital radius. These values are dependent on the type of impurity.[30] The impurity levels are localized discrete levels for low impurity concentrations. Above some critical concentration n_i the wave functions of neighboring impurities overlap and the impurity levels evolve into impurity bands. A rough estimate for the critical concentration for Bi-rich BiSb is n_i

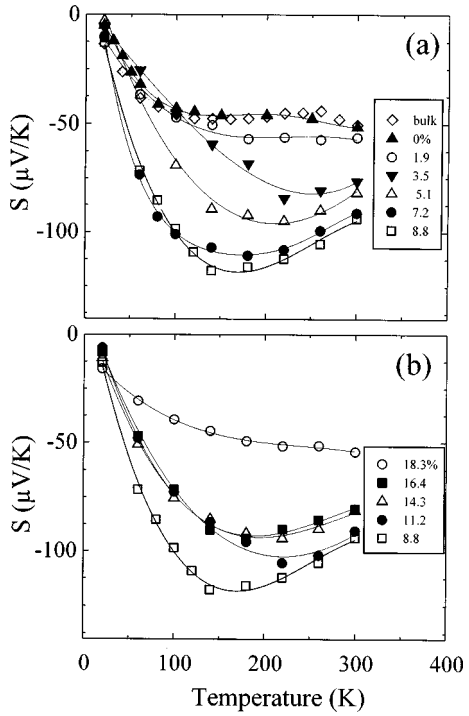

FIG. 3. TEP's of $Bi_{1-x}Sb_x$ alloy thin films as a function of temperature perpendicular to the trigonal axis. The 8.8% Sb alloy was graphed twice for comparison.

$\approx 1/(2r_1)^3 \approx 10^{12}\,\mathrm{cm}^{-3}$, which is rather low compared to a concentration $\sim 10^{19}\,\mathrm{cm}^{-3}$ required for Si. Thus this low critical impurity concentration estimate supports the possible presence of impurity bands in Bi-rich BiSb alloy thin films since the impurity concentrations are of the order $10^{16}\,\mathrm{cm}^{-3}$ for the highest purities available (99.9999%).

In Figs. 3(a) and 3(b), the TEP values for the $Bi_{1-x}Sb_x$ alloy thin films are plotted as a function of temperature between 20 and 300 K. The TEP of a pure Bi film is seen to be in good agreement with the previous single crystal values for conduction perpendicular to the trigonal axis as reported by Gallo, Chandrasekhar, and Sutter[33] and Korenblit, Kustretsov, and Shalyt.[34] The addition of Sb into Bi affects the TEP values. The 1.9% Sb alloy shows a slightly enhanced TEP. As the Sb concentration increases, the magnitude of the alloy TEP increases. The maximum TEP was obtained at 8.8% Sb alloy and thereafter decreases with a further increase in Sb composition, as shown in Fig. 3(b). The TEP values for the alloy thin films are seen to be larger than those for the pure Bi film. At low temperatures, the magnitude of the TEP increases linearly with increasing temperature as in bulk. For alloys with Sb concentrations between 3.5 and 16.4% reaches a peak at some intermediate temperature and the decreases at high temperature. However, the TEP of the 1.9 and 18.3% Sb alloy thin films shows a temperature dependence similar to that of pure Bi, in which no distinct peak is observed. For a thermoelectric material containing both electrons and holes, the total TEP may be modeled by the relation $S=(\sigma_e S_e+\sigma_p S_p)/(\sigma_e+\sigma_p)$, where σ_e and σ_p are the electrical conductivities and S_e and S_p are the TEP's for electrons and holes, respectively. The observed negative TEP implies a higher mobility for electrons than for holes (assuming $n=p$). The magnitude of the TEP increases with decreasing temperature above a certain temperature. This increase is due to the freeze-out of electrons and holes and an increase of the electron-to-hole mobility ratio with decreasing temperature, which depends on the Sb concentration. At low temperature, the magnitude of the TEP decreases linearly with decreasing temperature as in bulk, which is due to the greater degeneracy of the carrier populations.

For a nondegenerate intrinsic semiconductor, assuming the contributing bands are parabolic with the same density of states and that the carriers are scattered primarily by acoustic phonons, the electrical resistivity and TEP can be written as[30]

$$\rho=\rho_0 \exp\left(\frac{E_C-E_F}{k_B T}\right) \tag{4}$$

and

$$S=\frac{k_B}{e}\left(\frac{E_C-E_F}{k_B T}+B\right) \tag{5}$$

where ρ_0 is a constant and E_c, E_F, and B are conduction-band edge, Fermi energy, and scattering parameter, respectively. The term E_c-E_F can be expressed as

$$E_C-E_F=\tfrac{1}{2}(E_{g0}-AT), \tag{6}$$

where E_{g0} is the band gap at 0 K and A is a constant. Using Eqs. (4)–(6), the band gap can be extrapolated to 0 K. Equation (4) has been used to derive the thermal effective band gap in the semiconducting BiSb alloy system.[1–17] Strictly speaking, it is hard to apply the above formula directly to BiSb because acoustic phonon scattering does not dominate in the thin films at low temperatures and because there are multiple hole bands (at L, H, and T). The band which makes the dominant contribution to the temperature dependence of the resistivity depends on a complex interplay between the band gap, density of states, mobility, and temperature. However, for a simple and qualitative understanding of the BiSb alloy system we used the above simple model to interpret our results and to compare our results with the reported literature values for bulk material and thin films.

The fitted thermal band gaps using Eq. (4) are shown in Fig. 4, compared with similarly calculated literature values for bulk[1,6–8] and 1-μm-thick epitaxial thin films grown on $BaF_2(111)$.[16] As mentioned in the Introduction, the semiconducting behavior in bulk occurs at alloys compositions between 7 and 22% Sb with a maximum band gap (18–20 meV) at $x=0.15$. However, we have observed several differences relative to the bulk system. The 3.5 and 5.1% Sb alloys (corresponding to semimetals in bulk) show semiconducting behavior. The Sb concentration for the maximum band gap shifts to a lower Sb concentration, from 15% in bulk to 9%. It is seen that the effective band gaps of thin films grown on CdTe(111) are larger than the bulk values, with a maximum gap of 40 meV.

Figure 5 shows a comparison of the TEP between our thin films and bulk values as a function of Sb concentration at several temperatures. Three important points are evident: (i) The magnitude of the TEP of the alloys with Sb concentration of 3.5 and 5.1% increases with decreasing temperature above 220 K, indicative of semiconducting behavior. (ii) The Sb concentration for the maximum TEP has

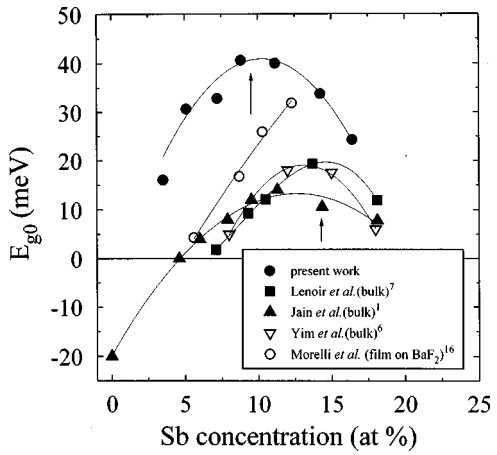

FIG. 4. Effective thermal band gap E_{g0} at 0 K as determined from temperature-dependent electrical resistivity measurement vs Sb concentration.

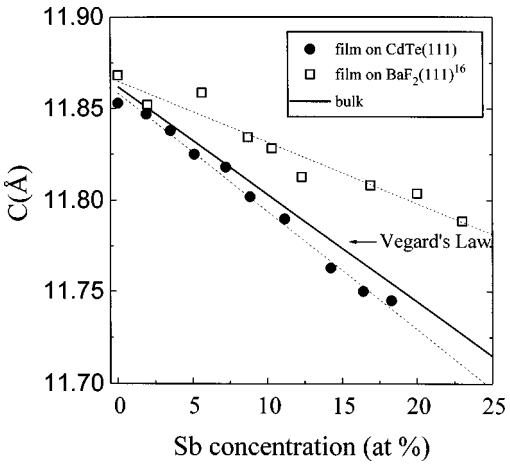

FIG. 6. The *c*-axis lattice constant in the hexagonal unit cell of $Bi_{1-x}Sb_x$ alloy thin films as a function of Sb concentration. The solid line gives results for bulk alloys.

shifted to lower Sb concentrations, from 15 to 9%. (iii) The TEP's of the alloy thin films grown on CdTe(111) are larger than for bulk alloys, which is consistent with an enhanced gap [see Eq. (5)]. All these differences observed in TEP measurements are consistent with the electrical resistivity results. In both transport measurements (electrical resistivity and TEP), the 8.8% Sb alloy has highest effective gap and the highest TEP. Using Eq. (5), we have fitted our TEP data to obtain effective band gaps. The overall behavior of the band gap with Sb concentration is quite similar to that determined by the temperature-dependent resistivity. The maximum band gap is $E_{g0}=35$ meV at 8.8% Sb as compared to $E_{g0}=40$ meV determined from the temperature-dependent electrical resistivity.

From the θ–2θ x-ray diffraction performed with a Matrix diffractometer (which utilizes a doubly-bent LiF crystal monocromator and Cu $K\alpha_1$ radiation) we can determine the *c*-axis lattice constant with respect to the hexagonal unit cell of BiSb, as shown in Fig. 6. For a given Sb concentration, the lattice constant for our films is consistently smaller than that of the bulk within scatter. The reproducibility of the substrate alignment is limited, resulting in few tenths of a degree deviation in 2θ, which leads to some scatter from the line drawn in Fig. 6. However, the general tendency of the *c*-axis lattice constants is toward smaller values than those of the bulk. From this trend we infer the presence of a tensile strain in our alloy films. This strain becomes larger with increasing *x*, since the lattice mismatch between BiSb and CdTe increases.

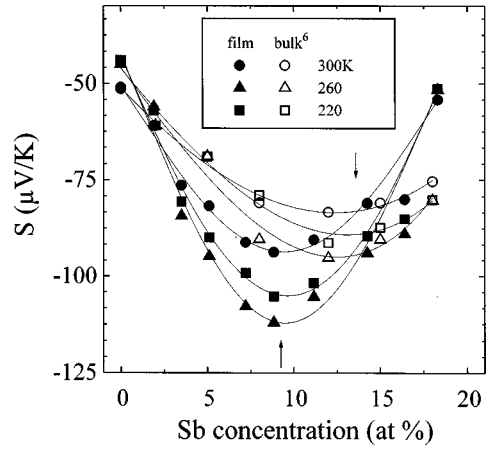

FIG. 5. TEP's of $Bi_{1-x}Sb_x$ alloy thin films and bulk crystal as a function of Sb concentration at several temperatures: 220, 260, and 300 K.

A possible explanation for the appearance of semiconducting behavior in the 3.5 and 5.1% Sb alloys, a shift in Sb concentration with maximum band gap and an enhanced effective band gap over bulk BiSb alloy, may be the strain effect, which modifies the electronic band structure, resulting in a shift of the relative position of the electron and hole bands. The semimetallic behavior of Bi and Sb is related to their rhombohedral $A7$ crystal structure. The $A7$ structure has two atoms per unit cell located at (u,u,u) and $(-u, -u, -u)$ and a rhombohedral angle α (for Bi, $u=0.237$ and $\alpha=57°14.2'$; for Sb, $u=0.233$ and $\alpha=57°6.5'$). Recently, total-energy all-electron relativistic band-structure calculations of the phase stability of bulk Bi were performed using the full-potential, linear, muffin-tin-orbital method.[35] It was demonstrated that the internal displacement leads to a stabilization of the observed $A7$ structure and drives a metal-semimetal transition in Bi. (Bi is a metallic for $u=0.25$.) In addition, the increase in the trigonal shear angle with internal displacement (to $u=0.237$) leads to a semimetal-to-semiconductor transition.[35] For $\alpha=60°$ (cubic), Bi becomes a direct bandgap semiconductor with the calculated gap of 30 meV at the *T* points. This calculation suggests that the dependence of the electronic structure on the Bi crystal structure provide a way of controlling the electronic structure. The presence of tensile strain in our films grown on CdTe(111) leads to an increase in the rhombohedral angle, which drives the electronic band structure of BiSb toward semiconducting behavior as mentioned above. The appearance of semiconducting behavior in the 3.5 and 5.1% Sb alloys, the shift of the Sb concentration for the maximum band gap, and the enhanced band gap over bulk BiSb alloys are all consistent with strain-altered band structure. On the other hand, Morelli, Partin, and Heremans[16] observed the slightly enhanced gap in BiSb alloy thin films grown on BaF_2(111) substrates. They attributed their enhanced band gap to a compressive strain caused by the smaller lattice

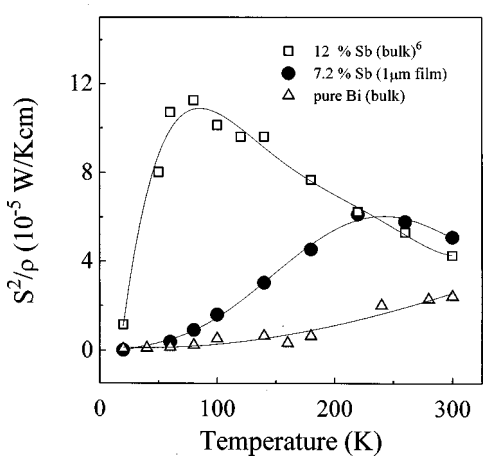

FIG. 7. Temperature dependence of the power factor (S^2/ρ).

constant of the substrate (4.38 Å). As shown in Fig. 6, the lattice constant for their films is consistently larger than that of the bulk. This is in contradiction with results of the band calculations of Shick, Freeman, and Ketterson. On the other hand, the large effect of hydrostatic pressure on the band structure of bulk Bi and BiSb alloys has been reported over a wide range of Sb concentrations. Both the L and T bands move up and down, depending on pressure and Sb concentration.[13]

To evaluate the suitability of BiSb alloy thin films for a thermoelectric module, we have plotted the power factor (S^2/ρ) as a function of temperature in Fig. 7. The temperature-dependent power factor for a 7.2% BiSb alloy thin film is compared to bulk Bi and $Bi_{0.88}Sb_{0.12}$ alloy crystals. Only the largest literature values are graphed in Fig. 7. These results show that power factors for the BiSb thin films peak at a significantly higher temperature (250 K) than for previous results for the bulk alloy (80 K). The peak temperature mainly depends on the electrical resistivity behavior. With a small band gap of 20 meV in bulk, the electrical resistivities of the alloys decreases with decreasing temperature below room temperature until a certain temperature, related to the thermal energy (e.g., at 300 K, $k_BT \sim 25$ meV). We observe that the 1.9, 3.5, 16.4, and 18.3 % alloys have a minimum in the resistivity below room temperature. However, for other films, e.g., 7.2% Sb alloy (having maximum power factor), the electrical resistivity increases with decreasing temperature. Therefore the peak occurs at a higher temperature. These results imply that thermoelectric properties, such as the optimum operating temperature and the magnitude of the figure of merit Z, depend on the magnitude of the band gap of the material and can be controlled by band engineering.

IV. CONCLUSION

We have studied the transport properties of MBE-grown 1 μm-thick $Bi_{1-x}Sb_x$ alloy thin films on CdTe(111)B over a wide range of Sb concentrations ($0 \leqslant x \leqslant 0.183$). Compared to the bulk alloy system, there are three important conclusions. (i) Semiconducting behavior was observed for the 3.5 and 5.1% Sb alloy thin films. (ii) The Sb concentration for the maximum TEP and thermal bandgap shifts toward lower Sb concentrations, from 15 to 9%. (iii) The effective thermal band gap and TEP's of the alloy thin films grown on CdTe(111) are larger than for bulk alloys. The differences between thin film grown on CdTe(111) and the bulk alloys may be due to strain modifying the electronic band structure. In addition, we have observed that the power factor S^2/ρ peaks at a significantly higher temperature (250 K) relative to that for the bulk alloy which peaks at (80 K). The dependence of the electronic structure on the Bi lattice parameters provides a means of controlling the electronic structure and thermoelectric properties of Bi and BiSb films by strains imposed by film/substrate lattice mismatch. These results suggest that band-engineered Bi-based materials may be useful in thermoelectric devices.

ACKNOWLEDGMENTS

We thank Dr. Igor Vurgaftman for a careful reading of the manuscript. This work was supported by ARPA under Grant No. MDA972-95-1-0020, by ONR under Document N0001496WX20241, and by DARPA under Grant No. DAAG55-97-1-0130. Use was made of MRL Central Facilities supported by the National Science Foundation, at the Materials Research Center of Northwestern University, under Grant No. DMR-9120521.

*Permanent address: Physics Department, HKUST, Clearwater Bay, Kowloon, Hong Kong, China.

†Also at Department of Electrical and Computer Engineering, Northwestern University, Evanston, Illinois 60208.

[1] A. L. Jain, Phys. Rev. **114**, 1518 (1959).

[2] S. Golin, Phys. Rev. **176**, 830 (1968).

[3] E. J. Tichovolski and J. G. Mavroides, Solid State Commun. **7**, 927 (1969).

[4] G. A. Mironova, M. V. Sudakaova, and Ta. G. Ponomarev, Fiz. Tverd. Tela **22**, 3628 (1980) [Sov. Phys. Solid State **22**, 2124 (1980)].

[5] G. Oelgart, G. Schneider, W. Kraak, and R. Herrmann, Phys. Status Solidi B **74**, K75 (1976).

[6] W. M. Yim and A. Amith, Solid-State Electron. **15**, 1141 (1972).

[7] B. Lenoir, M. Cassart, J.-P. Michenaud, H. Scherrer, and S. Scherrer, J. Phys. Chem. Solids **57**, 89 (1996).

[8] D. M. Brown and S. J. Silverman, Phys. Rev. **136**, A290 (1964).

[9] V. G. Alekseeva, N. F. Zaets, A. A. Kudryashov, and A. B. Ormont, Fiz. Tekh. Poluprovodn. **10**, 2243 (1976) [Sov. Phys. Semicond. **10**, 1332 (1976)].

[10] N. B. Brandt and E. A. Svistova, J. Low Temp. Phys. **2**, 1 (1970).

[11] N. B. Brandt and Ya. G. Ponomarev, Zh. Eksp. Teor. Fiz. **55**, 1215 (1968) [Sov. Phys. JETP **28**, 635 (1969)].

[12] N. B. Brandt, S. M. Chudinov, and V. G. Karavaev, Zh. Eksp. Teor. Fiz. **61**, 689 (1971) [Sov. Phys. JETP **34**, 368 (1972)].

[13] N. B. Brandt, Kh. Dittmann, and Ya. G. Ponomarev, Fiz. Tverd. Tela **13**, 2860 (1971) [Sov. Phys. Solid State **13**, 2408 (1972)].

[14] E. E. Mendez, A. Misu, and M. S. Dresselhaus, Phys. Rev. B **24**, 639 (1981).

[15] M. Lu, R. J. Zieve, A. van Hulst, H. M. Jaeger, T. F. Rosenbaum, and S. Radelaar, Phys. Rev. B **53**, 1609 (1996).

[16] D. T. Morelli, D. L. Partin, and J. Heremans, Semicond. Sci. Technol. **5**, S257 (1990).

[17] D. M. Brown and S. J. Silverman, Phys. Rev. **136**, A290 (1964).
[18] B. Y. Jin, H. K. Wong, G. K. Wong, J. E. Hilliard, and J. B. Ketterson, Thin Solid Films **110**, 29 (1983).
[19] A. Divenere, H. K. Wong, G. K. Wong, J. B. Ketterson, and J. E. Hilliard, J. Cryst. Growth **70**, 452 (1984).
[20] S. C. Shin, J. E. Hilliard, and J. B. Ketterson, J. Vac. Sci. Technol. A **2**, 296 (1984).
[21] D. L. Partin, J. Heremans, D. T. Morelli, C. M. Thrush, C. H. Olk, and T. A. Perry, Phys. Rev. B **38**, 3818 (1988).
[22] D. L. Partin, C. M. Thrush, J. Heremans, D. T. Morelli, and C. H. Olk, J. Vac. Sci. Technol. B **7**, 348 (1988).
[23] J. Heremans, D. L. Partin, C. M. Thrush, G. Karczewski, M. S. Richardson, and J. K. Furdyna, Phys. Rev. B **48**, 11 329 (1993).
[24] A. DiVenere, X. J. Yi, C. L. Hou, H. C. Wang, J. B. Ketterson, G. K. Wong, and I. K. Sou, Appl. Phys. Lett. **62**, 2640 (1993).
[25] A. DiVenere, X. J. Yi, C. L. Hou, H. C. Wang, J. Chen, J. B. Ketterson, G. K. Wong, J. R. Meyer, C. A. Hoffman, and F. J. Bartoli, J. Vac. Sci. Technol. B **12**, 1136 (1994).
[26] C. A. Hoffman, J. R. Meyer, F. J. Bartoli, A. DiVenere, X. J. Yi, C. L. Hou, H. C. Wang, J. B. Ketterson, and G. K. Wong, Phys. Rev. B **48**, 11 431 (1993); *ibid.* **51**, 5535 (1995).
[27] S. Cho, A. DiVenere, G. K. Wong, J. B. Ketterson, J. R. Meyer, and C. A. Hoffman, Solid State Commun. **102**, 673 (1997).
[28] S. Cho, A. DiVenere, G. K. Wong, J. B. Ketterson, J. R. Meyer, and J. I. Hong, Phys. Rev. B **58**, 2324 (1998).
[29] S. Cho, A. DiVenere, G. K. Wong, J. B. Ketterson, and J. R. Meyer, J. Vac. Sci. Technol. A **17**, 9 (1999).
[30] G. Busch and H. Schade, *Lectures on Solid State Physics* (Pergamon, New York, 1976), pp. 290–379.
[31] G. Wannier, Phys. Rev. **52**, 191 (1937).
[32] W. S. Boyle and A. D. Brailsford, Phys. Rev. **120**, 1943 (1960).
[33] C. F. Gallo, B. S. Chandrasekhar, and P. H. Sutter, J. Appl. Phys. **34**, 144 (1963).
[34] I. Ya. Korenblit, M. E. Kusnetsov, and S. S. Shalyt, Zh. Eksp. Teor. Fiz. **56**, 8 (1969) [Sov. Phys. JETP **29**, 4 (1969)].
[35] B. Shick, A. J. Freeman, and J. B. Ketterson, Bull. Am. Phys. Soc. **43**, 171 (1998).